

An experimental insight of friction stir welding of dissimilar AA 6061/Mg AZ 31 B joints

N Rajesh Jesudoss Hynes¹, M Vivek Prabhu², P Shenbaga Velu³ ,
R Kumar⁴ , R Tharmaraj⁵ , Muhammad Umar Farooq⁶ and
Catalin Iulian Pruncu⁷ 

Proc IMechE Part B:
J Engineering Manufacture
1–11

© IMechE 2021



Article reuse guidelines:

sagepub.com/journals-permissions

DOI: 10.1177/09544054211043474

journals.sagepub.com/home/pib



Abstract

In the present scenario, aerospace and automobile industries depend on lightweight materials such as magnesium and aluminum alloys because of their great balance between mechanical properties and weight ratio. Despite these benefits during the joining process of these dissimilar materials by welding, many challenges arise. The prominent one is related to the low melting points of these lightweight metals which make it almost impossible the joining using conventional arc welding techniques. To tackle this challenge, Friction Stir Welding (FSW) can be considered as a promising candidate tool. In this study, to demonstrate the FSW performances of joining two dissimilar materials we have investigated the joining of AA 6061 and Mg AZ 31 B using a built-in house a modified milling machine. The dissimilar combinations of AA 6061 and Mg AZ 31 B joints were successfully joined by embedding different welding conditions and varying the offset distance. The mechanical performances were evaluated by conducting specific mechanical tests such as micro-hardness, tensile, and impact tests, respectively. To explain the mechanical results, we have applied optical microscopy observation on the microstructure associated with the bonding location. The results prove that the strength of the Friction Stir Welded joints is much higher as compared to other techniques especially in terms of dissimilar metals.

Keywords

Friction stir welding, aluminum, magnesium, mechanical properties

Date received: 17 February 2021; accepted: 15 August 2021

Introduction

FSW is a solid-state welding process described as eco-friendly and energy-efficient technique. It was firstly proposed in 1991 by The Weld Institute (TWI). Since then, numerous researchers have worked to further develop and improve the FSW process. Meilinger and Török¹ revealed that it generates structures with superior strength compared to conventional welding, especially for joining aluminum alloys. Moreover, the use of FSW was also extended for polymers,² Fiber Reinforced Polymers,³ aluminum composites,⁴ magnesium,⁵ and steels.⁶

TWI describes this joining process by the use of a high-speed rotating Friction Stir Welding tool, which is plunged over the surface of contact between two workpieces that enable the joining. The high-speed rotating tool results in frictional heat which create a plasticized zone that forms around the tool. Once the plasticized zone is created, the tool moves gradually along the

¹Department of Mechanical Engineering, Mepco Schlenk Engineering College, Sivakasi, India

²Mechanical Department, Velammal College of Engineering and Technology, Madurai, India

³Department of Mechanical Engineering, PSR Engineering College, Sivakasi, India

⁴Department of Mechanical Engineering, Eritrea Institute of Technology, Asmara, Eritrea

⁵Institute of Fundamental Technological Research, Polish Academy of Sciences, Warsaw, Poland

⁶School of Mechanical Engineering, University of Leeds, Leeds, UK

⁷Design, Manufacturing and Engineering Management, University of Strathclyde Glasgow, Glasgow, UK

Corresponding authors:

Catalin Iulian Pruncu, Design, Manufacturing and Engineering Management, University of Strathclyde, Glasgow, Scotland G1 1XJ, UK.
Email: catalin.pruncu@strath.ac.uk

N Rajesh Jesudoss Hynes, Department of Mechanical Engineering, Mepco Schlenk Engineering College, Sivakasi 626005, Tamil Nadu, India.
Email: findhynes@yahoo.co.in

Muhammad Umar Farooq, School of Mechanical Engineering, University of Leeds, Leeds, LS2 9JT, UK.
Email: Umarmuf0@gmail.com

joining line formed by the two workpieces. During the movement of the FSW tool, a consolidated solid-phase joint is formed.⁷ Mishra and Ma⁸ studied the mechanisms and microstructural formation of FSW of aluminum alloys. It has been reported that a rotating tool used in this process, do not get consumed, which make this process mechanically stable. This tool has a unique design shoulder and pin that is inserted into the joining edges of the plates and moves gradually along the joint line.

The advances in technology require industries to integrate different materials combination for the final product.^{9–12} One such combination is aluminum and magnesium. The use in today's applications of magnesium alloys and aluminum alloys have increased rapidly. Therefore, the joining of these two different materials has become of prime importance these days. These alloys possess excellent corrosion-inhibiting properties and can be finished to a high degree of accuracy. Aluminum 6061-T6 alloy has strength nearly equal to that of mild steel. Due to its maturity, the fabrication process of the 6061-T6 aluminum sheet is cost-effective. Major applications of aluminum and magnesium were identified in truck bodies and frames, structural components, aircraft landing mats, and other lightweight applications. The ultimate strength of these materials is around 310 MPa while shearing strength is about 206 MPa.

Metals have been used in aviation and aerospace industries since a long time ago for both military and civil applications. To achieve fuel efficiency and reduce the emissions in air and spacecraft applications, the reduction in the weight of the components is a critical objective.^{13,14} This can trigger a reduction in their cost of operation too. However, the weight reduction in aluminum alloys is challenging, they also have limitation in terms of higher temperature ranges, which have a direct impact on damage properties. Due to these disadvantages, magnesium was found as a good alternative for application in aerospace industries. Major aerospace companies like Boeing used magnesium for their aircraft (e.g. 737, 747, 757, and 767) to make thrust reversers. It is also witnessed in applications of engines and transmission casings of helicopters. Magnesium and its alloys are found in spacecraft and missiles as well. During the design of an aircraft, great importance is given to the reduction of the weight of the Lift-off. Other notable advantages of magnesium include the capability to be exposed to ozone, good performances when subjected to the impact of high energy particles and their ability to withstand higher temperatures. The intercontinental ballistic missiles such as Titan, Atlas, and Agena use magnesium in significant quantities.^{15,16} It was noted that AA 6061 and AZ 31B are the two major materials found in aircraft which requires to be welded. Unfortunately, arc welding techniques could not be employed because they generate a thick brittle intermetallic compound at the joint interface.¹⁷ Hence, there is a

need to explore a better option from which one can be FSW which allows joining AA 6061 and Mg alloy.

The laser welding method used for joining Al-Mg alloys results in a great amount of intermetallic compound formation. It also leads to the formation of minute cracks in the welded specimen paving the way for the destruction of the bonding strength.¹⁸ On the other hand, fusion welding of dissimilar joints gives a minimum amount of bonding strength on the Aluminum-Magnesium joints.¹⁹ Generally, fusion welding cannot be used for joining Al-Mg joints, because there exists a great amount of intermetallic compound with forms at the interface of the weldment. Considerable efforts have been made to control the heat input and intermetallic formation at the joint interface produced with CMT welding of Al-Mg joints.²⁰ We speculate that nowadays the most suitable technique for joining dissimilar materials is friction stir welding. It helps to reduce the formation of intermetallic compounds because it can effectively control the amount of welding time and lower the heat input.

Yong et al.²¹ indicated that the Inter Metallic Compounds (IMCs) results in an uneven hardness distribution during FSW of 5052Al and AZ31Mg alloys, which may cause an early joint fracture. Yamamoto et al.²² stated that the tensile strength of the Al/Mg joint is mainly governed by the thickness of the IMCs layer and the mechanical interlocking of Al/Mg alloys. On the other hand, Rao et al.²³ revealed that the strong bonding in the NZ can be obtained due to the partial mechanical interlocking between Mg alloy and the IMCs layer. Firouzdor and Kou²⁴ stated that the joint strength can be improved by a long interface length and an inter-penetrating feature thickness. Therefore, the way to regulate and control the distribution characteristic of the IMCs at the Al/Mg interface which enable improving the mechanical properties has been becoming a research hotspot. Few assistive technologies such as ultrasonic have been widely applied to FSW, which provides many benefits, such as vibration and acoustic streaming. Chowdhury et al.²⁵ introduced an adhesive layer in magnesium-to-aluminum friction stir (FS) spot-welded joints. They noted that because an adhesive layer introduced in this process both quasi-static and fatigue strength of the joints were increased. Fu et al.²⁶ claimed that a weld joint with no defect was obtained, with a higher tensile strength, on the Mg plate side, once the Mg plate was placed on the advancing side with 0.3 mm offset toward the Mg alloy plate. It is possible by providing a combination of tool rotational speed in between 600 and 800 rpm and lowers travel speed 30–60 mm/min for joining of Al 6061-T6 to AZ31B-O alloys. Sameer and Birru²⁷ fabricated joint of AZ91 magnesium to AA6082(T6) aluminum alloys by FSW process with the help of a tapered cylindrical groove tool, which was manufactured from H13 steel metals. They suggested that whenever the Mg alloy is

placed on the advancing face, it produces a defect-free joint with a fine grain structure. But when Mg is placed on the retreating face, it forms crack and void defects, along with the formation of a brittle intermetallic compound because of improper mixing of metals. Ji et al.²⁸ indicated that the fracture propagation path is changed from along the IMCs at the Al/Mg interface of the conventional joint to across the Mg alloy during ultrasonic-assisted friction stir spot welding of Al/Mg alloys. Xueqi et al.²⁹ also pointed out that the ultrasonic exerted a little preheating effect on the welded workpieces, and hardly influenced the peak temperature during FSW of Al/Mg alloys. Therefore, there are major advantages of improving material flow and changing the form of the IMCs as well as without obvious temperature variation, which is promising fact and has huge potential to join Al/Mg alloys. When was analyzed the mechanical properties of the AA6061 Aluminum alloy joints by gas metal arc welding, gas tungsten arc welding, and friction stir welding, it was noted that the friction stir weld joints generated high strength values when compared with gas metal arc welding and gas tungsten arc welding.³⁰ Besides, a non-consumable high carbon steel tool was used for friction stir welding in this work. Xu et al.³¹ investigated the effect of base metal state on the microstructure and mechanical properties of Al-Mg-Si alloy friction stir-welded (FSW) joints. The result shows that aluminum grains and insoluble phases of the FSW joints were not affected by the BM state, but the compositions of the precipitated phases in the heat-affected zones (HAZs) and nugget zones (NZs) depended on the phase compositions of the base metals. Hu et al.³² studied the joint formation of aluminum/magnesium joints using ultrasonic stationary shoulder assisted friction stir welding process. They explored the mechanism formation, microstructure, and fracture behavior of dissimilar joints. Derazkola et al.³³ demonstrated the thickness of intermetallic layer is reduced due to submerge friction stir welding of Al/Mg joints and also a lower hardness is attained that can be improved by processing in warm water. Zhang et al.³⁴ studied the mechanism of defects formation upon UFSW of AA2219 aluminum alloy. They demonstrated that the welding defects could occur at both low- and high rotation speeds, but under an optimum condition, the tensile strength may reach 80% of that of AA2219 alloy and an improvement in the hardness of stir zone (SZ). Heirani et al.³⁵ studied UFSW of Al5083 alloy and showed that improved tensile strength and hardness are achievable. Kumar et al.³⁶ examined the maximum amount of intermetallic compound formed at the aluminum/magnesium joints. They observed that maximum tensile strength is achieved with a joint efficiency of 61%. Maciel et al.³⁷ proposed hybrid friction stir welding to improve the damage tolerance and also substantial strength of Al/Mg joints. Choi et al.³⁸ indicated that with a lower welding speed, the average grain diameter in the Mg stir zone of the Ti/Mg joints became smaller even

though the higher welding temperature and lower strain rate. Mehta et al.³⁹ claimed that no diffusion layer was initiated in the magnesium side in Friction Stir Welded Al/Mg joints. The tensile strength of the dissimilar joints is enhanced by cooling assisted welding process due to the reduction in the number of intermetallic compounds inside the weld bead. Zheng et al.⁴⁰ examined the microstructure and mechanical properties of self-reaction assisted friction stir welding of aluminum 5052/AZ31B Mg joints. The result shows that sound weld joints were produced without noticeable welding defects such as cracks were obtained.

By evaluating various dissimilar material joining process, it can be highlighted that FSW has the most remarkable development in the recent past. This is because of good flexibility, eco-friendly benefits, and being an efficient energy technology also termed as “Green Technology.” FSW uses much lower energy when it is compared with other joining techniques. To further gain more insight into this technique, in the present research we have evaluated systematically the weldability of the two most used alloys, AA 6061 and Mg AZ31B, in aerospace and naval application due to their lightweight characteristics. The experimental protocol embedded in this research which links the mechanical and microstructural characterization allows us to fundamentally understand the materials mechanism behavior dictated by FSW. These results are paramount important for the lightweight industry (aerospace, automotive) and computation community to validate their numerical models and create robust manufacturing procedures.

Materials and method

Workpiece materials

Aluminum 6061 is a heat-treatable alloy with medium to high strength and have better properties than 6005A. Even though the strength of these alloys at the weld zone is relatively low but they have excellent corrosion resistance. The fatigue strength of these alloys is in the medium range. The cold formability of the alloy is superior at temper T4 but limited at temper T6 condition. However, for complex cross-sections, the suitability of the alloy is not well-ranked. On the other hand, the machinability of Magnesium alloys is easy and are lightweight materials. Their corrosion resistance can be increased through anodizing. The Magnesium AZ31B is easily available in the desired forms such as bar, sheet, and plate. Since, the strength to weight ratio is higher, they are a viable option for the replacement of aluminum alloys. This grade is widely available and used in several applications as compared to other types.

Tool design and materials

The major function of a tool is to heat the material by friction and stir the material to produce sound welds.

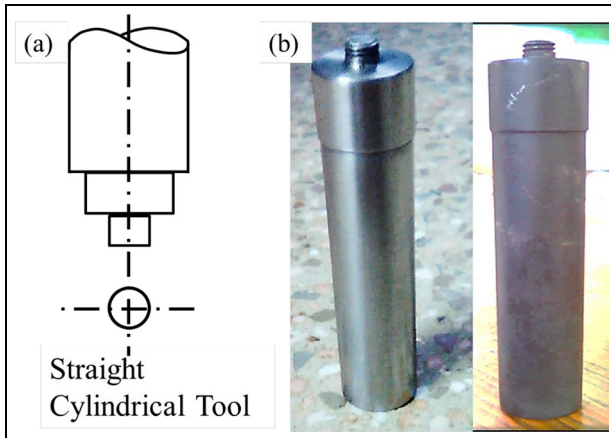


Figure 1. (a) Schematic of FSW tool adapted after⁴² and (b) machined and hardened tool.

The tool has two major components (a) pin and (b) shoulder. Based on the size and shape of the two there is a vast classification of the tools. Normal tools have step turnings with shoulder diameter larger than the pin diameter. Nevertheless, during the welding of harder alloys like titanium and steel, the tool of the FSW is facing serious stress and higher temperatures are attained. Due to the reduced life of the FSW tool, nowadays, their application is limited commercially.³⁵ A review on the tool design was performed by Rai et al.⁴¹ while investigating the heat generation phenomenon.

The present work is concerned with Aluminum and Magnesium alloys in which tool steel is recommended due to its cost effectiveness. Generally, the tool material must have the following requirements:

- It must have a red hardness to withstand the temperatures in the range 300°C–450°C.
- It must have enough Tungsten content to bear the forces.
- It must have an optimum amount of Chromium; because lower amount of Chromium lessens the corrosion resistance properties.
- It must have less Cobalt content since it causes the aluminum to adhere to the tool; the thermal stress of the tool could be affected by the coefficient of thermal expansion.

Both high carbon steel and HSS M2 steel would satisfy the requirements. Since HSS has high machinability and red hardness compared to high carbon steel it was selected for the tool fabrication.

For welding of Aluminum and Magnesium, the main factors affecting the weld structures were investigated. Few researchers^{26,29} explored the thickness ratio on the formation of the stir zone by varying the tool diameter. They also studied the properties of FS welded AA6061 and AZ31B after carrying out the tensile test on the welded samples. They have concluded that the tensile properties are higher when the diameter of the shoulder

is around 21 mm and it is relatively lower for the rest of the diameters analyzed. In this work, the shoulder diameter of the tool was varied from 12 to 24 mm (two to four times the plate thickness). Threaded pin profile made of HSS would not wear at the working temperature and it would not wear since the welded materials are soft. Moreover, it provides a substantial stirring force. The pin length was 4 mm and its diameter was 8 mm with threads of pitch of 1 mm. Thus, the tool was machined to the dimension. After machining the tool had a hardness of 42 HRC. It needed to be heat treated to obtain good hardness. The friction stir welding tool schematic and an actual tool are shown in Figure 1(a) and (b).

Experimentation

To carry out the experimentation, a vertical milling machine was modified to perform the butt configured FSW of Aluminum and Magnesium joints. The modified experimental setup and process schematic are shown in Figure 2. The machine is issued with a 5HP motor, which has a sturdy solid bed and a varying speed bed type milling machine. The feed rate was precisely controlled in all the x , y , and z -axes. The speed of the rotating spindle on the machine was set as constant in 500 rpm in order to vary and test the other parameters. Table 1 shows process conditions whereas Table 2 displays the specifications of process parameters used to develop the friction stir welded joints. The levels of process parameters are selected on the basis of literature recommendations and premature experiments for better fundamental investigation (as recommended method in literature).^{43,44} The cross-section of the dissimilar joint between Aluminum/Magnesium alloys was polished and then etched for microstructural examination using sand-papers and etched with ferric chloride solution. The microstructure of the joint interface was analyzed using optical microscope Quantax 200 with X-Flash – Bruker having an operating voltage of 200 kV and a scanning electron microscope (Carl Zeiss EVO 18).

Results and discussion

Tensile testing

The friction stir welded samples after tensile testing are shown in Figure 3. Tests were conducted in Electronic Universal Testing Machine, UTES-10 (India) having a 100 kN capacity and the specimen was prepared as per ASME8 standard. The fractured specimens are shown in Figure 4. From this, the influence of rotational speed on the tensile strength and percentage elongation of the friction stir welded samples could be predicted. The base material of AA 6061 alloy demonstrated an ultimate tensile strength of about 290 MPa which is slightly higher than the base material of Mg-AZ31 B alloy (about 260 MPa).

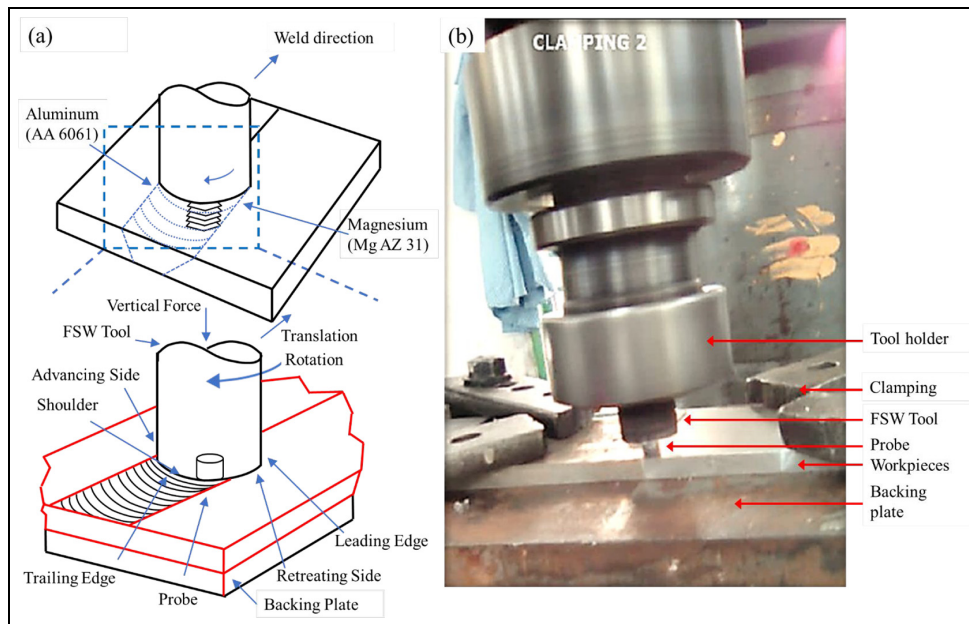


Figure 2. Pictorial view of setup: (a) process schematic adapted after⁴⁵ and (b) actual experimentation setup.

Table 1. Combinations and specifications of trials.

Trail experiment no.	Combinations	Specifications
1	AA 6061-Mg AZ31B	Spindle speed: 500 rpm, advancing side: aluminum, feed: 3 mm/min
2	AA 6061-Mg AZ31B	Spindle speed: 500 rpm, advancing side: aluminum, feed: 8 mm/min
3	Mg AZ31B-Mg AZ31B	Spindle speed: 500 rpm, feed: 30 mm/min, weld line: center, both sides: magnesium
4	AA 6061-AA 6061	Spindle speed: 500 rpm, feed: 20 mm/min, weld line: center, both sides: aluminum
5	Mg AZ31B-AA 6061	Spindle speed: 500 rpm, advancing side: aluminum, feed: 10 mm/min, weld line: center

Table 2. Process parameters for welding experiments.

Parameters	Values
Spindle speed	500 rpm
Feed rate (AA 6061-Mg AZ31B)	3, 8, 10 mm/min
Feed rate (MgAZ31B-Mg AZ31B)	30 mm/min
Feed rate (AA 6061-AA6061)	20 mm/min
Dwell time	6 s
Rotation direction	Clockwise
FSW control	Vertical direction

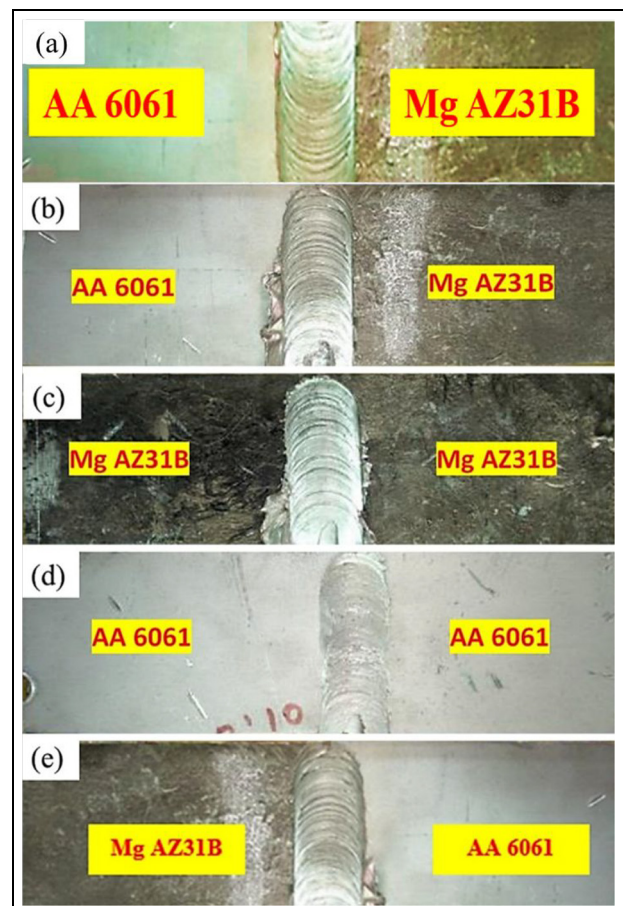


Figure 3. Friction stir welded joints: (a) AA 6062 and Mg AZ31B (feed 3 mm/min), (b) AA 6062 and Mg AZ31B (feed 8 mm/min), (c) Mg AZ31B-Mg AZ31B, (d) AA 6061-AA 6061, and (e) Mg AZ31B-AA 6061.





Specimen	Tensile tested Image	Ultimate Tensile strength and Percentage of elongation	Position of Fracture
AA 6061-Mg AZ31B (Specimen 1)		39 MPa, 2 %	5mm from the centre (in the TMAZ)
Mg AZ31B- Mg AZ31B (Specimen 2)		88 MPa, 1.8 %	7mm from centre (in the HAZ)
AA 6061- AA 6061 (Specimen 3)		123 MPa, 5.8 %	3mm from the centre (in TMAZ)
AA 6061- Mg AZ31B (Specimen 4)		37 MPa, 3.5 %	6mm from the centre (in the TMAZ)

Figure 4 Specimen after tensile test.

Moreover, the aluminum joint showed the highest strength compared to the magnesium itself. Also, aluminum has higher elongation in all direction due to the higher value of Young's modulus (68.9 GPa) compared to Magnesium (45 GPa). The friction stir welded plates demonstrated the elongation of 2% for specimen 1, 1.8% for specimen 2, 5.8% for specimen 3, and 3.5% for specimen 4. Moreover, this elongation was probably driven by the spindle speed of about 500 rpm, which finally enabled a maximum elongation of about 5.8% for similar aluminum joints. The maximum tensile strength achieved during the tensile test is about 123 MPa imposing a spindle speed of 500 rpm and

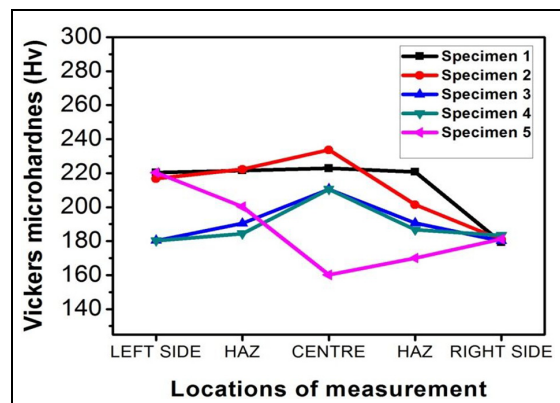


Figure 5. Microhardness profile of the different welded specimen.

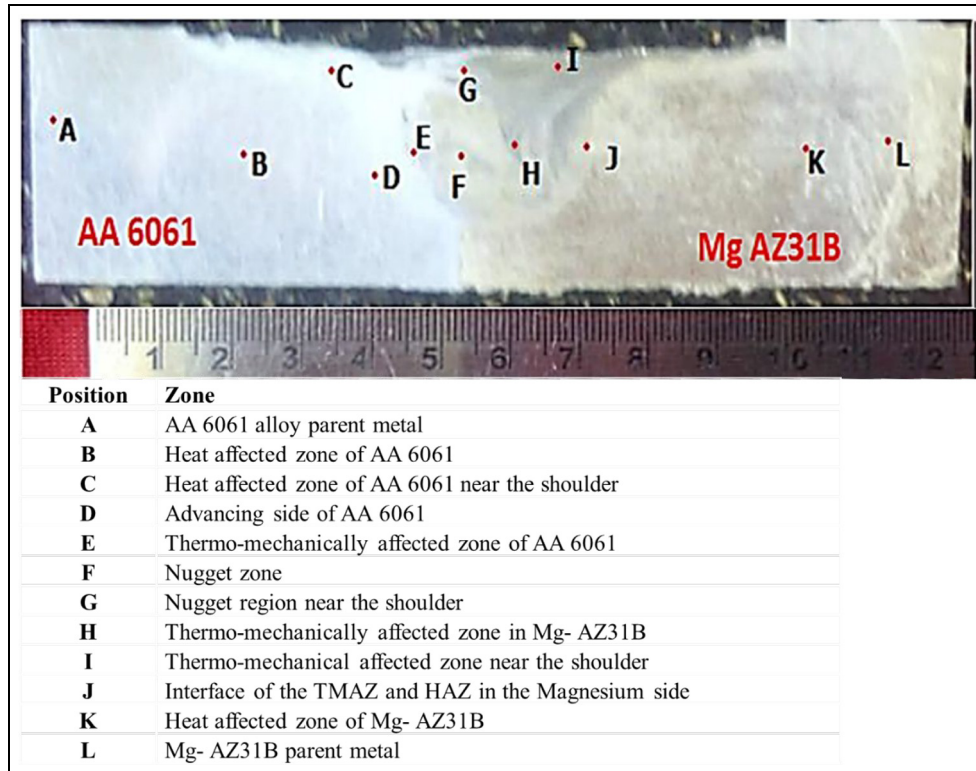


Figure 6. Friction Stir Welded AA 6061-Mg AZ31B joint and positions of microstructure at the interfacial region.

20 mm/min feed rate. This is about 42.41% of the tensile strength of AA 6061 alloy.

Microhardness

Microhardness measurements were carried out using Micro Vickers indentation method by applying 100 g load for 10 s as per ASTM E92 standard on a Micro Vickers Hardness Testing Machine, Blue Star India). Machine capable to obey a force ranging from 10 to 1 kg.

The consequence of the FSW on the distribution of hardness on the welded samples at a rotational speed of 500 rpm is shown in Figure 5. It presents the measured hardness values across both directions from HAZ, center, and on the transverse cross-section of the friction stir welded joints. The center zone of friction stir welded (specimen 1, specimen 2, specimen 3, and specimen 4) has exhibited a maximum level of hardness due to the stirring action. The hardness profiles inside the weld zone are highly dependent on the processing parameters which are controlled by the heat input, fusion zone dilution, molten pool circulation, intermixing of dissimilar metals, and subsequent formation and distribution of intermetallic phases within the Mg- and Al-rich interaction zones. This is because there is no mechanical deformation (stirring); however, the peak temperature reached is enough to soften the material near the stir/nugget zone as Sample 5.

Microstructure investigation

Figure 6 shows the image of AA 6061-Mg AZ31B joint obtained at the processing parameters of 500 rpm, with the feed rate of 8 mm/min. The different positions are selected for microstructural examination after friction stir welding are listed in Figure 7. This examination allows further understanding of the behavior of friction stir welding. We selected this condition because at the spindle speed of 500 rpm, the heat generated was high enough to weld and produce the material flush successfully. This microstructure analysis is performed on the aluminum-magnesium weld with an weld-line offset toward magnesium. Microstructures were captured for the points noted as shown in Figure 6.

The cross-section of the defect-free weld joint alone was analyzed using optical microscopy. The base material microstructure of AA6061 and AZ 31B consists of grains of unequal size and distribution. WE speculated that the microstructure in the shoulder influenced the region between the Al alloy base material and the stir zone. The grain size can be seen to decrease at the transition with the base material.^{46,47} There is then a sharp demarcation where it passes into the stir zone. We can see clearly the grain size in the 6061-T6 material being away from the transition zone. The “A” region is denoted as the Friction stir processed region. It is far off from the center and it has a relatively lower temperature compared to the nugget zone at the time of welding. It has magnesium silicide (Mg_2Si) particles

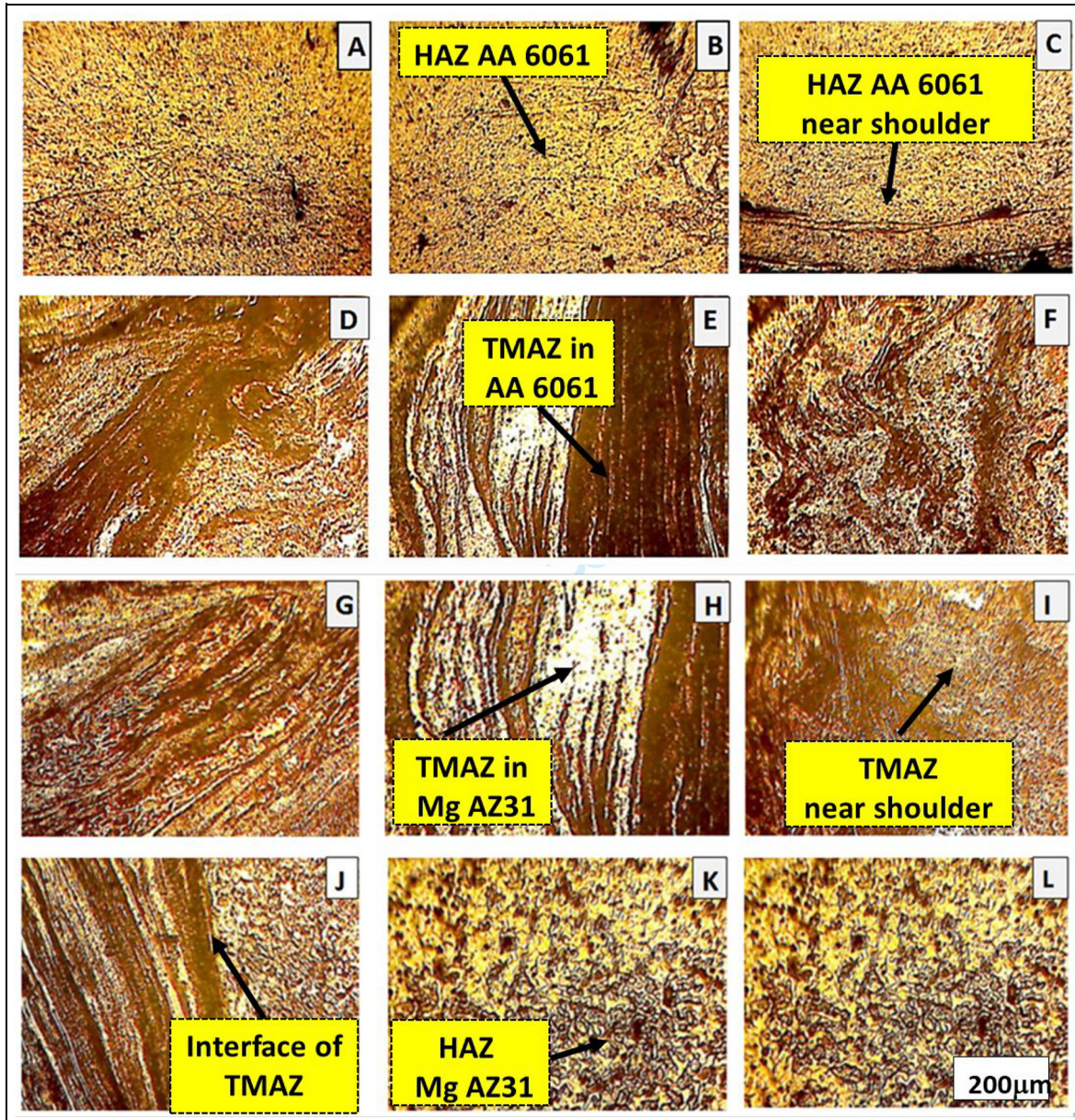


Figure 7. Microstructure at various zones of Friction stir welded joint: (a) AA 6061 parent metal, (b) heat affected zone of AA 6061, (c) heat affected zone of AA 6061 near shoulder, (d) advancing side of AA 6061, (e) thermo-mechanically affected zone in AA 6061, (f) nugget zone, (g) nugget region near shoulder, (h) thermo-mechanically affected zone in Mg AZ31B, (i) thermo-mechanically affected zone near the shoulder, (j) interface of thermo-mechanically affected zone and heat affected zone in Mg AZ31B side, (k) heat affected zone in Mg AZ31B, and (l) Mg AZ31B parent metal.

since Al6061 has a higher concentration of Mg and Si next to Aluminum. The region “B” is denoted as the heat-affected zone of AA 6061. We have noted that in the heat-affected zone particles size of Mg_2Si precipitate are increased. There was found no plastic deformation in this zone but there exists a thermal cycle. The region “C” is denoted as a heat-affected zone of aluminum near the shoulder. In this region, the coarsened precipitate of Mg_2Si is reduced to fine grains. Since at the shoulder, the temperature is high and it stirs at a higher speed.

The region “D” is denoted as the advancing side of the aluminum. In this region, the magnesium on the

other side is stirred into the Aluminum side. This zone shows elongated grains since they are in the thermo-mechanical affected zone (TMAZ). The region “E” is denoted as the thermo-mechanically affected zone of AA 6061. This is the transition zone between the heat-affected zone (HAZ) and the nugget zone. It has a highly deformed structure. There is minimum of strain deformation of TMAZ, yet there is no recrystallization in this area, however it undergoes plastic deformation. The region “F” is considered as the nugget zone. This zone has recrystallized crystals of aluminum and magnesium with very fine size. Recrystallization occurs in this region due to the very high temperature.^{48–50} The

region “G” is denoted as the nugget region near the shoulder. In this region, the basin-shaped nugget zone is produced. The region “H” is denoted TMAZ in magnesium. WE suspected it since the Magnesium is on the retreating side of the nugget zone. The grains are not as sharp as in the advancing side. The region “I” is denoted as TMAZ near the shoulder. It is bounded by the nugget zone. The region “J” is denoted as the interface of the TMAZ and HAZ in the magnesium side. Therefore, in this region, the TMAZ and HAZ can be clearly distinguished. The region “K” is denoted as the heat-affected zone of Mg-AZ31B. In the HAZ of magnesium, precipitates of $Mg_{13}Al_{17}$ can be found. The region “L” is denoted as the parent metal of magnesium. In this region, a small number of precipitates $Mg_{12}Al_{17}$ were notes as brittle.

We found in this research that the weld metal is composed of columnar crystals and some dendrite crystals which are in contrasts to the microstructures of the gas tungsten arc welded dissimilar joints of the Mg-Al presented in Kumar et al.³⁶ and Jawad et al.⁴³ Here, the dynamic recrystallization (DRX) facilitates the solid-state flow which promoted a superior FSW.^{51,52} Probabaly the adiabatic heat arising from the deformation-induced DRX contributed to the weld zone temperatures which reached approximately 0.8TM (TM is the melting point of the material). In turn it generated for the weld zone an intercalated microstructures, with lamellar-like shear bands rich either in Al or Mg.^{53,54}

Conclusion

In this work Friction stir welding of AA 6061/Mg AZ31B dissimilar metals was investigated. Surface integrity, tensile strength, and microhardness were investigated by varying feed rates. Based on the results and discussions on the rigorous characterization of AA 6061/Mg AZ31B joints produced through friction stir welding, the following conclusions could be extracted:

1. A non-consumable cost-effective tool made of tool steel for aluminum and magnesium ensured the fulfillment of objective related to heat production and dissemination. Suppression of excessive heat input has shown to improve joint integrity by limiting IMC growth and adequacy of cooling rate which further can be improved through assistive technologies.
2. From the dissimilar welding, the welding of dissimilar materials has relatively coarse grains in the nugget zone. Joint integrity was classified through the cross-sectional welding interface producing distinct boundary and slight evidence of lamellar structure.
3. Most of tensile test specimens was fractured at the TMAZ zone due to the absence of recrystallization, corroborated to a lesser extent of strains and

strain rates as well as a lower peak temperature. This research can be further extended by investigating the underwater FSW process in order to improve the tensile strength.

4. Weld line offset from center was responsible for the accumulation of higher concentration of magnesium. This reduces the Inter Metallic Compounds and thus enabled a higher tensile strength (39 MPa), for the offset center line, compared to center of FSW (37 MPa).


Declaration of conflicting interests

The author(s) declared no potential conflicts of interest with respect to the research, authorship, and/or publication of this article.

Funding

The author(s) received no financial support for the research, authorship, and/or publication of this article.

ORCID iDs

P Shenbaga Velu  <https://orcid.org/0000-0001-7963-5671>
 R Kumar  <https://orcid.org/0000-0002-7910-9142>
 R Tharmaraj  <https://orcid.org/0000-0001-6494-7664>
 Catalin Iulian Pruncu  <https://orcid.org/0000-0002-4926-2189>

References

1. Meilinger Á and Török I. The importance of friction stir welding tool. *Prod Process Syst* 2013; 6(1): 25–34.
2. Arora A, De A and DebRoy T. Toward optimum friction stir welding tool shoulder diameter. *Scr Mater* 2011; 64(1): 9–12.
3. Kumar R, Singh R and Ahuja IPS. Friction stir welding of 3D printed melt flow compatible dissimilar thermoplastic composites. *Proc IMechE, Part C: J Mechanical Engineering Science* 2021; 235(10): 1878–1890.
4. Iqbal MP, Vishwakarma RK, Pal SK, et al. Influence of plunge depth during friction stir welding of aluminum pipes. *Proc IMechE, Part B: J Engineering Manufacture*. Epub ahead of print 23 August 2020. DOI: 10.1177/0954405420949754.
5. Rose AR, Manisekar K and Balasubramania V. Influences of tool rotational speed on tensile properties of friction stir welded AZ61A magnesium alloy. *Proc IMechE, Part B: J Engineering Manufacture* 2012; 226(4): 649–663.
6. Elyasi M, Aghajani Derazkola H and Hosseinzadeh M. Investigations of tool tilt angle on properties friction stir welding of A441 AISI to AA1100 aluminium. *Proc IMechE, Part B: J Engineering Manufacture* 2016; 230(7): 1234–1241.
7. Chiteka K. Friction stir welding/processing tool materials and selection. *Int J Eng Res Technol* 2013; 2(11): 8–18.
8. Mishra RS and Ma ZY. Friction stir welding and processing. *Mater Sci Eng R Rep* 2005; 50: 1–78.
9. Nandan R, DebRoy T and Bhadeshia H. Recent advances in friction-stir welding–process, weldment

- structure and properties. *Prog Mater Sci* 2008; 53(6): 980–1023.
10. Saeidi M, Manafi B, Besharati Givi M, et al. Mathematical modeling and optimization of friction stir welding process parameters in AA5083 and AA7075 aluminum alloy joints. *Proc IMechE, Part B: J Engineering Manufacture* 2016; 230(7): 1284–1294.
 11. Ghetiya ND and Patel KM. Welding speed effect on joint properties in air and immersed friction stir welding of AA2014. *Proc IMechE, Part B: J Engineering Manufacture* 2017; 231(5): 897–909.
 12. Palanivel R, Laubscher R, Vigneshwaran S, et al. Prediction and optimization of the mechanical properties of dissimilar friction stir welding of aluminum alloys using design of experiments. *Proc IMechE, Part B: J Engineering Manufacture* 2018; 232(8): 1384–1394.
 13. Sato YS, Harayama N, Kokawa H, et al. Evaluation of microstructure and properties in friction stir welded superaustenitic stainless steel. *Sci Technol Weld Join* 2009; 14(3): 202–209.
 14. ul Haq MA, Hussain S, Ali MA, et al. Evaluating the effects of nano-fluids based MQL milling of IN718 associated to sustainable productions. *J Clean Prod* 2021; 310: 127463.
 15. Lee W-B, Lee C-Y, Kim M-K, et al. Microstructures and wear property of friction stir welded AZ91 Mg/SiC particle reinforced composite. *Compos Sci Technol* 2006; 66(11–12): 1513–1520.
 16. Kiss Z and Czirány T. Applicability of friction stir welding in polymeric materials. *Period Polytech Mech Eng* 2007; 51(1): 15–18.
 17. Zhang YN, Cao X, Larose S, et al. Review of tools for friction stir welding and processing. *Can Metall Q* 2012; 51(3): 250–261.
 18. Liu L and Wang H. Microstructure and properties analysis of laser welding and laser weld bonding Mg to Al joints. *Metall Mater Trans A* 2011; 42(4): 1044–1050.
 19. Marya M, Edwards G, Marya S, et al. Fundamentals in the fusion welding of magnesium and its alloys. In: *Proceedings of the seventh JWS international symposium*, Kobe, Japan, 2001, pp.20–22.
 20. Zhang H, Hu S, Wang Z, et al. The effect of welding speed on microstructures of cold metal transfer deposited AZ31 magnesium alloy clad. *Mater Des* 2015; 86: 894–901.
 21. Yong YAN, Zhang D-T, Cheng QIU, et al. Dissimilar friction stir welding between 5052 aluminum alloy and AZ31 magnesium alloy. *Trans Nonferrous Met Soc China* 2010; 20: s619–s623.
 22. Yamamoto N, Liao J, Watanabe S, et al. Effect of intermetallic compound layer on tensile strength of dissimilar friction-stir weld of a high strength Mg alloy and Al alloy. *Mater Trans* 2009; 50(12): 2833–2838.
 23. Rao HM, Yuan W and Badarinarayan H. Effect of process parameters on mechanical properties of friction stir spot welded magnesium to aluminum alloys. *Mater Des (1980–2015)* 2015; 66: 235–245.
 24. Firouzidor V and Kou S. Al-to-Mg friction stir welding: effect of material position, travel speed, and rotation speed. *Metall Mater Trans A* 2010; 41(11): 2914–2935.
 25. Chowdhury SH, Chen DL, Bhole SD, et al. Lap shear strength and fatigue behavior of friction stir spot welded dissimilar magnesium-to-aluminum joints with adhesive. *Mater Sci Eng A* 2013; 562: 53–60.
 26. Fu B, Qin G, Li F, et al. Friction stir welding process of dissimilar metals of 6061-T6 aluminum alloy to AZ31B magnesium alloy. *J Mater Process Technol* 2015; 218: 38–47.
 27. Sameer MD and Birru AK. Mechanical and metallurgical properties of friction stir welded dissimilar joints of AZ91 magnesium alloy and AA 6082-T6 aluminium alloy. *J Magnes Alloys* 2019; 7(2): 264–271.
 28. Ji S, Li Z, Zhang L, et al. Effect of lap configuration on magnesium to aluminum friction stir lap welding assisted by external stationary shoulder. *Mater Des* 2016; 103: 160–170.
 29. Xueqi L, Yang C and Wu C. Experimental investigation on ultrasonic vibration enhanced FSW of Al-Mg dissimilar materials. *J Mech Eng* 2016; 52: 58–64.
 30. Lakshminarayanan AK, Balasubramanian V and Elangovan K. Effect of welding processes on tensile properties of AA6061 aluminium alloy joints. *Int J Adv Manuf Technol* 2009; 40(3–4): 286–296.
 31. Xu ZZ, Liu CY, Zhang B, et al. Effects of base metal state on the microstructure and mechanical properties of Al–Mg–Si alloy friction stir-welded joints. *J Manuf Process* 2020; 56: 248–257.
 32. Hu W, Ma Z, Ji S, et al. Improving the mechanical property of dissimilar Al/Mg hybrid friction stir welding joint by PIO-ANN. *J Mater Sci Technol* 2020; 53: 41–52.
 33. Derazkola HA, Eyvazian A and Simchi A. Submerged friction stir welding of dissimilar joints between an Al-Mg alloy and low carbon steel: thermo-mechanical modeling, microstructural features, and mechanical properties. *J Manuf Process* 2020; 50: 68–79.
 34. Zhang HJ, Liu HJ and Yu L. Microstructure and mechanical properties as a function of rotation speed in underwater friction stir welded aluminum alloy joints. *Mater Des* 2011; 32(8–9): 4402–4407.
 35. Heirani F, Abbasi A and Ardestani M. Effects of processing parameters on microstructure and mechanical behaviors of underwater friction stir welding of Al5083 alloy. *J Manuf Process* 2017; 25: 77–84.
 36. Kumar U, Acharya U, Saha SC, et al. Microstructure and mechanical property of friction stir welded Al-Mg joints by adopting modified joint configuration technique. *Mater Today Proc* 2020; 26: 2083–2088.
 37. Maciel R, Bento T, Braga DF, et al. Fatigue performance of friction stir weld-bonded Al-Mg joints. *Procedia Struct Integr* 2019; 17: 949–956.
 38. Choi J-W, Liu H, Ushioda K, et al. Effect of an Al filler material on interfacial microstructure and mechanical properties of dissimilar friction stir welded Ti/Mg joint. *Mater Charact* 2019; 155: 109801.
 39. Mehta KP, Carlone P, Astarita A, et al. Conventional and cooling assisted friction stir welding of AA6061 and AZ31B alloys. *Mater Sci Eng A* 2019; 759: 252–261.
 40. Zheng B, Hu X, Lv Q, et al. Study of self-reaction assisted friction stir welding of AZ31B Mg/5052 Al alloys. *Mater Lett* 2020; 261: 127138.
 41. Rai R, De A, Bhadeshia HKDH, et al. Review: friction stir welding tools. *Sci Technol Weld Join* 2011; 16(4): 325–342.
 42. Mohanty HK, Venkateswarlu D, Mahapatra MM, et al. Modeling the effects of tool probe geometries and process parameters on friction stirred aluminium welds. *J Mech Eng Autom* 2012; 74–79.

43. Jawad M, Jahanzaib M, Ali MA, et al. Revealing the microstructure and mechanical attributes of pre-heated conditions for gas tungsten arc welded AISI 1045 steel joints. *Int J Press Vessels Piping* 2021; 192: 104440.
44. Khan SA, Rehman M, Farooq MU, et al. A detailed machinability assessment of DC53 steel for die and mold industry through wire electric discharge machining. *Metals* 2021; 11(5): 816.
45. Choi WJ, Morrow JD, Pfefferkorn FE, et al. The effects of welding parameters and backing plate diffusivity on energy consumption in friction stir welding. *Procedia Manuf* 2017; 10: 382–391.
46. Verma S and Misra JP. Effect of process parameters on temperature and force distribution during friction stir welding of armor-marine grade aluminum alloy. *Proc IMechE, Part B: J Engineering Manufacture* 2021; 235(1–2): 144–154.
47. Song M and Kovacevic R. Numerical and experimental study of the heat transfer process in friction stir welding. *Proc IMechE, Part B: J Engineering Manufacture* 2003; 217(1): 73–85.
48. Gao J, Li C and Shen Y. Investigations into the mechanical, morphological and thermal analyses of friction stir processing of high-density polyethylene composites. *Proc IMechE, Part B: J Engineering Manufacture* 2018; 232(7): 1193–1200.
49. Zhou X, Mackenzie D and Pan W. A new distributed cooling method for mitigating residual stress in friction stir welding. *Proc IMechE, Part B: J Engineering Manufacture* 2016; 230(12): 2204–2213.
50. Gadakh VS and Kumar A. Friction stir welding window for AA6061-T6 aluminium alloy. *Proc IMechE, Part B: J Engineering Manufacture* 2014; 228(9): 1172–1181.
51. Biswas P, A Kumar D and Mandal NR. Friction stir welding of aluminum alloy with varying tool geometry and process parameters. *Proc IMechE, Part B: J Engineering Manufacture* 2012; 226(4): 641–648.
52. Kasman Ş and Kahraman F. Investigations for the effect of parameters on the weld performance of AA 5083-H111 joined by friction stir welding. *Proc IMechE, Part B: J Engineering Manufacture* 2014; 228(8): 937–946.
53. Zhang H, Huang JH, Lin SB, et al. Temperature simulation of the preheating period in friction stir welding based on the finite element method. *Proc IMechE, Part B: J Engineering Manufacture* 2006; 220(7): 1097–1106.
54. Alhourani A, Awad M, Nazzal MA, et al. Optimization of friction stir back extrusion mechanical properties and productivity of magnesium AZ31-B seamless tubes. *Proc IMechE, Part B: J Engineering Manufacture*. Epub ahead of print 8 May 2021. DOI: 10.1177/09544054211014465.